DFUB 2000/19
Bologna, December 4, 2000

Limits on radiative decays of solar neutrinos from a measurement during a solar eclipse.

S. Cecchini[1,2], G. Giacomelli[1,4], R. Giacomelli[1], D. Haşegan[3], O. Mariş[3], V. Popa[1,3], R. Serra[4,5], M. Serrazanetti[6], L. Ştefanov[3], L. Tasca[5] and V. Văleanu[3]

[1]*Sezione INFN, 40127 Bologna, Italy*
[2]*Istituto TESRE del CNR, 40129 Bologna, Italy*
[3]*Institute of Space Sciences, Bucharest R-76900, Romania*
[4]*Dip. di Fisica, Università degli Studi, 40126 Bologna, Italy*
[5]*Dip. di Astronomia, Università degli Studi, 40127 Bologna, Italy*
[6]*Osservatorio Astronomico, 40017 San Giovanni in Persiceto (BO), Italy*

ABSTRACT

A search for possible radiative decays of solar neutrinos with emission of photons in the visible range was performed during the total solar eclipse of August 11, 1999. Due to very bad weather conditions our two telescopes were unable to collect useful data; fortunately we obtained several video camera images from a local TV station. An analysis of the digitised images is presented and limits on the lifetime for radiative decay are discussed.

1. Introduction

It is generally agreed that most probably neutrinos have non–zero masses. This belief is based primarely on the evidence/indication for neutrino oscillations from data on solar and atmospheric neutrinos.

Neutrino oscillations are possible if the flavour eigenstates are not pure mass eigenstates, e.g.:

$$|\nu_e >= |\nu_1 > \cos\theta + |\nu_2 > \sin\theta \tag{1}$$

where $m_{\nu_2} > m_{\nu_1}$ and θ is the mixing angle.

Since few years there is evidence that the number of solar neutrinos arriving on Earth is considerably smaller than what is expected on the basis of the "Standard Solar Model" and of the "Standard Model" of particle physics, where neutrinos are massless (see e.g. [1]). One possible explanation of these experimental results involves neutrino oscillations, either in vacuum with $\Delta m^2_{sun} = m^2_{\nu_2} - m^2_{\nu_1} \sim 10^{-10}$ eV^2 (as originally discussed in [2, 3]) or resonant matter oscillations $\Delta m^2_{MSW} \sim 10^{-5}$ eV^2 [4, 5].

Recent results from Super-Kamiokande [6], MACRO [7] and Soudan2 [8] experiments on atmospheric neutrinos support the hypothesis of neutrino oscillations (in particular $\nu_\mu \to \nu_\tau$) with large mixing ($\sin^2 2\theta > 0.8$) and $\Delta m^2_{atm} \simeq 3 \times 10^{-3}$ eV^2.

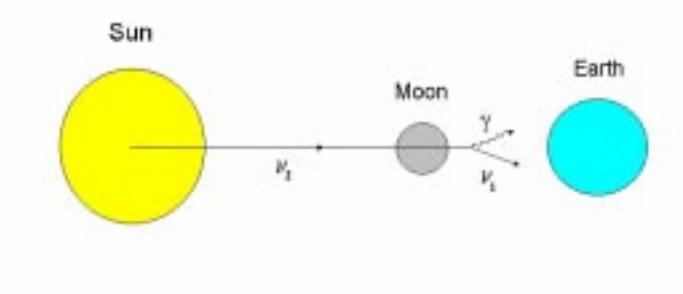

Figure 1: Sketch of the principle of the experiment to detect radiative neutrino decays during a solar eclipse (the emission angles of the photon and of the neutrino are enlarged).

Another indication in favor of neutrino oscillations with a third energy scale $\Delta m^2_{LSND} \simeq 1$ eV^2 is reported in [9].

The above observations appear to be the first indications for new physics beyond the "Standard Model", and any model that generates neutrino masses must contain a natural mechanism that explains their values and the relation to the masses of their corresponding charged leptons.

Different scenarios have been proposed to explain all the observations, including the results with neutrinos from reactors and accelerators [10, 11, 12].

If neutrinos do have masses, then the heavier neutrinos could decay into the lighter ones. For neutrinos with masses of few eV the only decay modes kinematically allowed are radiative decays of the type $\nu_i \rightarrow \nu_j + \gamma$ (where lepton flavour would be violated).

Upper bounds on the lifetimes of such decays are based on astrophysical non–observation of the final state γ rays. Limits were obtained from measurements of X and γ ray fluxes from the Sun [13] and SN 1987A [14, 15].

In the case of neutrinos with nearly degenerated masses, of the order of the eV, the emitted photon can be in the visible or ultraviolet bands [16, 17, 18]. A first tentative to detect such photons, using the Sun as a source, was made during the total solar eclipse of October 24, 1995 [18].

Direct visible photons from the Sun come at a rate of some 10^{17} cm^{-2} s^{-1}; this makes a direct search for photons from solar neutrino decays impossible. To perform a measurement one must take advantage of a total solar eclipse, which cuts by at least 8 orders of magnitude the direct photon flux. By looking with a telescope at the dark disk of the Moon one can search for photons emitted by neutrinos decaying during their 380000 km flight path from the Moon to the Earth, Fig. 1.

In this paper we describe the methodology employed for such a search and give limits obtained from a preliminary measurement performed during the total solar eclipse of 11 August, 1999.

2. Kinematics of radiative decays

We assume the existence of a possible neutrino radiative decay, $\nu_2 \rightarrow \nu_1 + \gamma$, where $m_{\nu_2} > m_{\nu_1}$ and ν_1, ν_2 are neutrino mass eigenstates.

The energy of the emitted photon in the earth reference laboratory system is

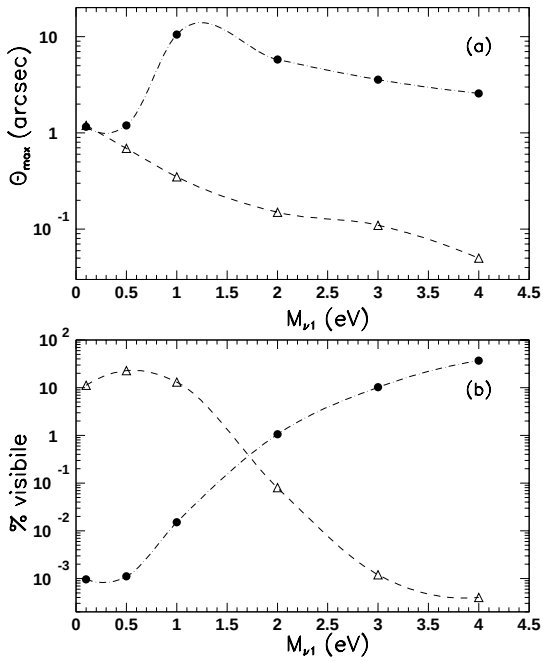

Figure 2: (a) Expected maximum angle of emission of visible photons from radiative solar neutrino decays as function of the ν_1 mass. (b) Percentage of visible photons for different ν_1 mass values. The open triangles correspond to the Super Kamiokande solution with $\Delta m^2 = 6 \times 10^{-6}$ eV^2 and $\sin^2 2\theta = 4 \times 10^{-3}$; the black points correspond to the solution with $\Delta m^2 = 2 \times 10^{-4}$ eV^2 and $\sin^2 2\theta = 0.71$.

$$E_{lab} = E_{cm}\gamma_\nu \left(1 + \beta_\nu \cos\theta^*\right) \tag{2}$$

where E_ν and $\gamma_\nu = \frac{E_\nu}{m_{\nu_2}} = (1 - \beta_\nu^2)^{-\frac{1}{2}}$ are in the lab. frame, and θ^* and E_{cm} are the photon emission angle and the energy of the emitted photon in the decaying neutrino rest frame.

For radiative neutrino decays the general expression for the angular distribution of the emitted photons in the rest frame of the parent neutrino is [19]

$$\frac{dN}{d\cos\theta^*} = \frac{1}{2}\left(1 - \alpha\cos\theta^*\right) \tag{3}$$

where the α parameter is equal to -1, +1, for left–handed and right–handed Dirac neutrinos, respectively, and 0 for Majorana neutrinos.

In order to estimate the expected number of photons in the visible range and the maximum angle of emission of visible photons from radiative solar neutrino decays we performed Monte Carlo simulations for neutrino masses in the range $0.1 - 4$ eV and two different scenarios of

solar neutrino oscillations ($\Delta m^2 = 2 \times 10^{-4}$ eV^2 and $\sin^2 2\theta = 0.71$; $\Delta m^2 = 6 \times 10^{-6}$ eV^2 and $\sin^2 2\theta = 3.98 \times 10^{-3}$). We used the following procedure:

i) randomly generate the quadrimomentum of ν_2 with reference to the solar neutrino energy spectra [20];
ii) randomly generate $\cos\theta^*$ by using Eq. 3 with $\alpha = -1$, in agreement with the Standard Model; the angular distributions in the lab. (earth) frame were found to be essentially insensitive to the choice of the α parameter [21];
iii) associate to each photon a quadrimomentum from the energy–momentum conservation;
iv) transform the computed values to the laboratory (earth) reference system.

Fig. 2 is the result of 5×10^8 simulated radiative decays, for each (m_{ν_1}, Δm^2) set of values.

3. The experiment

We implemented an experiment designed to make observations during the total solar eclipse of August 11, 1999 (NOTTE, Neutrino Oscillations with Telescope during the Total Eclipse) . The aim was to exploit the possible visible photons emitted in $\nu_2 \to \nu_1 + \gamma$ decays, during the solar neutrino flight from the Moon to the Earth and the shielding of the direct solar light by the Moon disk.

We intended to use two optical telescopes: a 25 cm Newtonian installed in the Parâng Massif in Romania, close to the point of maximum eclipse; and a smaller one (12.5 cm Cassagrain) mounted on an automatic pointing device in a MIG–29 supersonic fighter of the Romanian Air Force. The airborne telescope would have had the advantages, compared to the ground one, of longer observation times [21] and of reduced light absorption and diffusion in the atmosphere, thus enlarging the detectable photon energy range.

The telescopes were equipped with CCD's and co–axial digital TV cameras for the control of the alignment. The expected overall integrated acceptance (1.3×10^5 cm^{2}s) [21] could allow an improvement of factor at least 20 relative to previous trial [18].

The extremely bad weather conditions made the observations impossible. We only had the possibility to use a SVHS video record offered to us by the television of Râmnicu Vâlcea; we obtained 2750 frames that allowed us to test our procedure for the extraction of a possible signal in the digitized frames.

The SVHS video was obtained with a Panasonic M9000 camera with a focal length of 200 mm and a diameter of 49 mm. The video was digitized using a 450 MHz Pentium II with 256 MByte RAM and a video card Marvel G200 with complex video imput and a CoDec (Compression/Decompression) hardware MJPEG which allowed a maximum resolution of 704×576, with compression of the frames. The used video player was a Panasonic NVHS1000 (standard SVHS) with all the connections in Y/C. The maximum resolution we were able to obtain without compressing the frames was 352×288 pixels.

We selected images of 32×32 pixels centered in the center of the Moon; the final image was the sum of the reduced 2747 available frames (in the following we shall refer to it as the *measured image*).

4. The analysis procedure

We used the measured image to test our data reduction software. The measured image is dominated by the image of the Moon in the solar light reflected by the Earth. In order to test this hypothesis we calculated the linear correlation coefficient between our measured image and

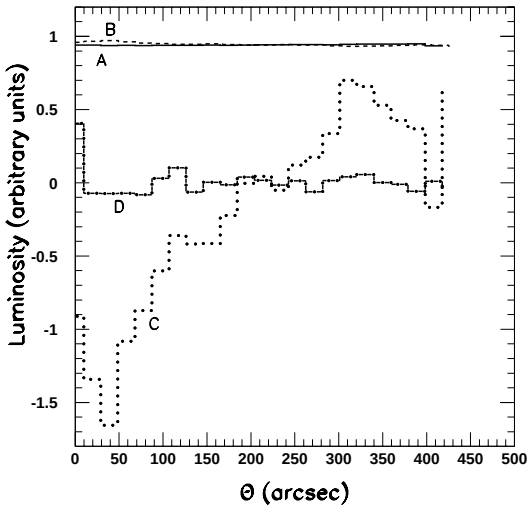

Figure 3: Procedure for trying to detect a radiative decay signal in the white channel. We give the average luminosity (arbitrary units) as a function of θ in arcsec for: A, the normalized measured image; B, the normalized image of the Moon from the Pises observatory; C, the image after subtraction (= measured–Pises); D, the 4^{th} order wavelet decomposition image.

a CCD image of the full Moon (obtained by a group of the Pises observatory [22]), from which we selected the same central region; we used the formula

$$C(x,y) = \frac{\sum_{i,j}(x_{i,j} - \bar{x})(y_{i,j} - \bar{y})}{\sqrt{\sum_{i,j}(x_{i,j} - \bar{x})^2 \sum_{i,j}(y_{i,j} - \bar{y})^2}}, \tag{4}$$

where the matrix elements $x_{i,j}$ and $y_{i,j}$ are the luminosities in each pixel of the two images.

We obtained a value $C(x,y) \simeq 0.6$, which implies that the two images are positively correlated and that we can thus substract one from the other (in the following we shall refer to this as the image after subtraction).

We tested this result by repeating the correlation analysis using the Moon image [22] and 10^6 images randomly generated in accordance with the light distribution in our measured TV image; the 10^6 images were generated via a Monte Carlo simulation using the HBOOK routine HRNDM [23]. We found that the linear correlation coefficient distribution is narrowly centered around zero, indicating that the correlation between our measured image and the Pises image of the Moon is not accidental.

We performed an intensity and contrast normalization, by imposing that the pixels average intensity and the lowest and the maximum pixel intensity values were the same for the two images. This procedure was independently applyed in all (red, green, blue and white) channels.

On the image after subtraction we made a fourth order wavelet decomposition. Fig. 3 illustrates our procedure in the white light; this procedure was performed in all color channels. In this way we atenuated any signal component (zodiacal light, corona light, etc. diffused by the atmosphere) on a scale greater than 2×2 pixels.

The expected signal from neutrino radiative decays is concentrated in the central pixel of about 20 arcsec. Neutrinos produced through thermonuclear reactions in the inner region of the Sun come from a relative small spatial volume corresponding in angular size to about 0.6% of

the Sun diameter (~ 12 arcsec); the maximum emission angles for visible photons, with respect to the initial neutrino flight direction, would always be limited to few arcsec (see Fig. 2).

5. Estimate of the lifetime sensitivity

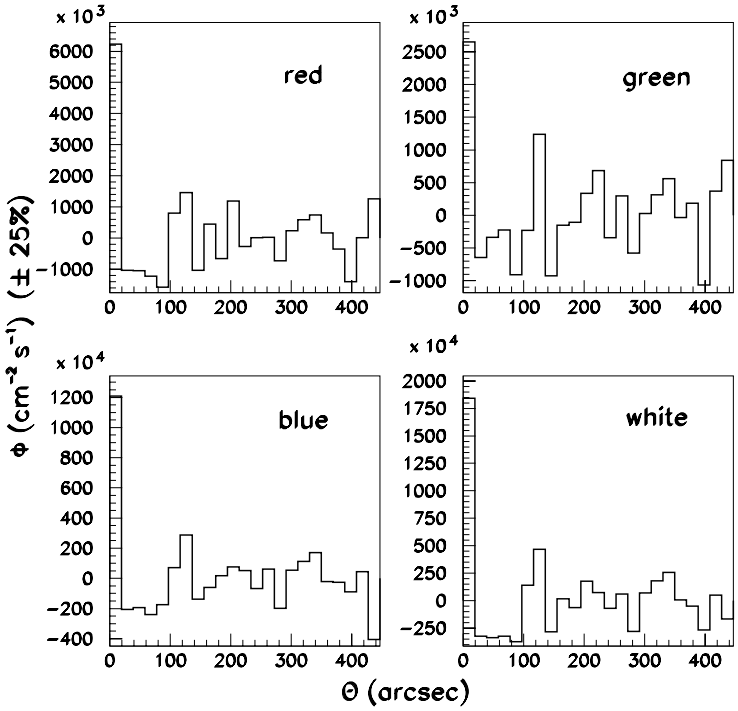

Figure 4: Average residual light fluxes, after moon subtraction and wavelet decomposition, in the red, blue, green channels and summed (white) expressed in photons cm^{-2} s^{-1} as a function of the angular distance from the center of the Moon disk expressed in arcsec.

In order to estimate the lifetime of ν_2 (see Eq. 5) we need to determine the flux of visible photons from $\nu_2 \to \nu_1 + \gamma$ decay. We performed a wavelet decomposition on the image after subtraction in all color channels.

The wavelet analysis is generally used in order to restore the image and to eliminate spurious signals. We were interested in what is usually considered as "noise"; thus we did not use the terms of wavelet decomposition but we used the residues; in particular we used the fourth order residuals of a wavelet decomposition in the Haar basis [24]; the fourth order is the highest usable order because the subtracted image has dimensions 32×32 pixels [1].

Fig. 4 shows the residuals light signal Φ, after wavelet decomposition, in the red, green, blue and white channels as a function of the distance from the center of the Moon disk. At the beginning of our analysis the 4^{th} order residual flux of the wavelet decomposition was expressed in Acquisition Digital Units (ADU). We made a conversion from ADU to photon flux units

[1]We recall that if the original image has 32×32 pixels, the 1^{th} order image has 2×2 pixels, ..., the 4^{th} order image has 16×16 pixels.

using the intensity profile of the solar corona. We used as calibration curve the intensity profile of the solar corona taken by a team from the Pises Observatory [22] during the same total solar eclipse. It presents two landmarks: the intensity of a lunar sea (12100 ADU) and of the Tycho crater (38800 ADU). We constructed the intensity profile of the solar corona for our measured image of the eclipse of August 11, 1999 in the red, green, blue and white channels as a function of the angular distance from the center of the Sun.

Note that the intensity profiles differ one from the other in the ordinate scale because the ADU is a unit which depends on the instrumental characteristics.

In order to estimate the conversion factor between the two ADU scales we interpolated the solar corona intensity profiles, both in our measured image and in the Pises image, with a cubic polynomial, and then we integrated them from 1.1 $R_\odot$ to 1.5 $R_\odot$. We obtained a ratio of conversion, f=(Pises ADU)/(our ADU)= 8.25.

The brightness of the full Moon, observed outside the atmosphere, when the Moon is at its apogee and the Earth is at its mean distance from the Sun, is $B = (0.34 \pm 0.01)$ lux. It corresponds to $N_\gamma = (140.0 \pm 4.4) \times 10^9$ photons cm^{-2} s^{-1} at an average wavelength of 5500 $\mathring{A}$. We assigned to this luminosity the intermediate value between the two reported on the Pises intensity profile; we estimate an error of about 25% on the conversion factor.

Fig. 4 shows that after the moon image removal and the wavelet decomposition of the remaining signal, a peak survived in the central pixel only. A conventional optical phenomenon that could lead to such a signal is the so called "Poisson spot" (a consequence of the Fresnel diffraction).

The diffraction occurs if the distance from the light source (the Sun) to an opaque disk (the Moon) or from a disk to a screen is much larger than the disk diameter and if the disk is much larger than the wavelength; it consists in the appearance of a luminous spot in the centre of the shadow (Poisson spot).

For a point source the intensity of the Poisson spot should be the same as the intensity that would be induced by the source at the distance of the screen; for plane waves the intensity of the spot is a quarter of that value. In our case it is difficult to estimate the expected intensity of the Poisson spot, as the Sun is an extended light source. Considering the light along a line perpendicular to an opaque circular disc, we expect to see darkness immediately behind the disc; the relative intensity should increase with increasing distance between the disc and the point of observation.

The contribution of the Poisson spot to the peaks in Fig. 4 can be estimated using the property that the intensity of the Poisson spot should not depend on the wavelength. Thus the ratios between the different Poisson intensities in different color channels should be the same as the ratios between the intensity recorded in similar conditions in the same channels of the solar spectrum.

Later we recorded the solar spectrum with a TV–camera similar to the Râmnicu Vâlcea one, and digitized the image in the same way as the measured eclipse image.

The TV–camera was equipped with a CCD, which had three different physical pixels for every pixel of the image: the first pixel is without filter while the others have red and blue filters. The green channel is obtained from a subtraction from the white signal of the summed red and blue ones; so it is in fact useless for the analysis described below.

From the solar spectrum frames we obtained a maximum signal of 56 ADU in the red field and of 88 ADU in the blue field; both with a background of 14 ADU. Fig. 4 gives in the central

m_{ν_1} (eV)	Δm^2 (eV)^2	$\sin^2 2\theta$	τ (s) Earth sys.	τ_0 (s) proper time
0.1	6×10^{-6}	4×10^{-3}	5.9×10^3	1.8×10^{-3}
0.5	6×10^{-6}	4×10^{-3}	1.2×10^4	1.9×10^{-2}
1	6×10^{-6}	4×10^{-3}	6.9×10^3	2.1×10^{-2}
1	2×10^{-4}	0.71	1.6×10^3	5.0×10^{-3}
2	2×10^{-4}	0.71	1.3×10^5	0.8
3	2×10^{-4}	0.71	1.3×10^6	12.0
4	2×10^{-4}	0.71	4.7×10^6	57.8

Table 1: Preliminary lifetime lower limits for a possible radiative decay of solar neutrinos, obtained from the 1999 total eclipse images. The limits are given as a function of m_{ν_1}, Δm^2 and $\sin^2 2\theta$. In the first three columns are given the oscillation parameters used to obtain the limits presented in the last two columns.

pixel a flux $\Phi^r_\gamma = 7.4 \times 10^6$ cm^{-2} s^{-1} in the red channel and $\Phi^b_\gamma = 1.4 \times 10^7$ cm^{-2} s^{-1} in the blue one.

We ascribe to the Poisson spot all the signal in the red channel; thus in the blue channel we obtain a residual photon flux of about $\sim 7\%$ of the signal.

We assume that the relative contribution to the overall decay signal in the white light may be taken as the average of the signals at the two extremities of the visible spectrum, that is 3.5% of the white maximum, thus $\Phi^w_\gamma = 7.4 \times 10^5$ cm^{-2} s^{-1}.

Preliminary results on the limits of the ν_2 lifetime, with respect to its radiative decay in the earth reference system, may be computed from

$$\Phi^w_\gamma = \epsilon \Phi_\nu \sin^2 2\theta \left(1 - e^{\frac{t_{M\to E}}{\tau}}\right) e^{\frac{t_{S\to M}}{\tau}} \tag{5}$$

where $\Phi_\nu = 8.56 \times 10^{10}$ cm^2 s^{-1} is the solar neutrino flux at the Earth computed from the Solar Standard Model, ϵ is the Monte Carlo branching fraction of visible photons produced in the radiative decay (see Fig. 2), θ is the neutrino mixing angle, $t_{S\to M}$ and $t_{M\to E}$ are the average flight times of solar neutrinos (assuming an average energy of about 325 eV) from the Sun to the Moon and from the Moon to the Earth, respectively.

The obtained preliminary lifetime lower limits on a possible radiative decay of solar neutrinos are given in Table 1. The limits are given as function of m_1, Δm^2 and $\sin^2 2\theta$.

The data did not allow to obtain lifetime limits for all mass–Δm^2 combinations. This suggests an underestimation of the contribution of the Poisson spot and of other background sources; thus the lifetime limits in Tab. 1 are conservative lower limits.

6. Conclusions

The analysis of the digitised images measured by a video camera used during the total solar eclipse of August 11, 1999 gave us the opportunity to test our data reduction software and also lead to some interesting results:

a) we evidenced the presence in our data of the Moon image in the light reflected from the Earth;

b) after the Moon image removal and the wavelet decomposition of the remaining signal we obtained a correlation function (luminosity versus distance from the center of the Moon) consistent with Fresnel diffraction (Poisson spot);

c) after removal of the Poisson spot contribution we obtain preliminary results on the limits of the ν_2 lifetime, see Tab. 1.
Experimental data of higher quality are needed to obtain more stringents limits.

8. Acknowledgments

The NOTTE experiment was partially supported by NATO Grant CRG.LG 972840. Special thanks are due to the Romanian Air Force for their co-operation. We gratefully acknowledge the Romanian Television of Râmnicu Vâlcea for providing us with their TV recording. We are indebted to many colleagues for discussions and advises. We acknowledge T. Franceschini of ITeSRE/CNR for help with the electronics.

References

[1] J.N. Bahcall, Solar Neutrinos: What Next?, hep–ex/0002018.

[2] V.N. Gribov and B.M. Pontecorvo, Phys. Lett. **B28** (1969) 493.

[3] B.M. Pontecorvo, Sov. Phys. Lett. **JETP 26** (1969) 984.

[4] L. Wolfenstein, Phys. Rev. **D17** (1978) 2369.

[5] S.P. Mikheyev and A. Yu. Smirnov, Yad. Fiz. **42** (1985) 1441; Nuovo Cim. **9C** (1986) 17.

[6] Super–Kamiokande Coll., Y. Fukuda et al., Phys. Rev. Lett. **81** (1998) 81; Phys. Rev. Lett. **82** (1999) 2644; Phys. Lett. **B467** (1999) 185.

[7] MACRO Coll., M. Ambrosio et al., Phys. Lett. **B434** (1998) 451; Phys. Lett. **B357** (1995) 481; Phys. Lett. **B478** (2000) 5.

[8] Soudan2 Coll., W.W.M. Allison et al., Phys. Lett. **B449** (1999) 137.

[9] LSND Coll., C. Athanassopoulus et al., Phys. Rev. Lett. **7** (1996) 3082.

[10] F. Boehm, Review of Neutrino Physics at Reactors, in 8^{th} Int. Workshop on Neutrino Telescopes, M. Baldo Ceolin ed., (Venezia, 1999) I, 311.

[11] M. Mezzetto, Neutrino Physics at Accelerators, in 8^{th} Int. Workshop on Neutrino Telescopes, M. Baldo Ceolin ed., (Venezia, 1999) I, 317.

[12] G. Giacomelli, Closing lecture at the 1999 S. Miniato Workshop, hep-ex/0001008.

[13] G.G. Raffelt, Phys. Rev. **D31** (1985) 3002.

[14] J.A. Frieman, Phys. Lett. **B200** (1988) 115.

[15] L. Chupp, Phys. Rev. Lett. **62** (1989) 505.

[16] J. Bouchez et al., Phys. Lett. **B207** (1988) 217.

[17] L. Oberauer, Nucl. Phys. **B28A** (1992) 165.

[18] C. Birnbaum et al., Phys. Lett. **B397** (1997) 143.

[19] G.R. Raffelt, Stars as Laboratories for Fundamental Physics, Univ. of Chicago Press (Chicago, 1996).

[20] J.N. Bahcall and M.H. Pinsonneault, Rev. Mod. Phys. **67** (1995) 781-808.

[21] S. Cecchini et al., Search for Neutrino Radiative Decays during the 1999 Total Solar Eclipse, 8^{th} UN/ESA Workshop on Basic Space Science, Mafraq, Jordan, 13-17 March 1999, Astroph. Space Sci. (2000), in press.

[22] http://www.astrosurf.prg/saturne/pises/ Eclipse99/Eclipse99.html.

[23] HBOOK, CERN Program Library Long Writeup Y250, CERN Geneva, Switzerland.

[24] A. Haar, Zur Theorie der orthogonalen Funktionensysteme, Math. Ann. **69** (1910) 331-371.